Supplementary Information (SI) for Materials Advances.

Enhanced piezo-response of mixed-cation copper perovskites with Cl/Br halide engineering

Amr Elattar[a,b,c*], Christopher Munoz[a], Libor Kobera[d], Andrii Mahun[d], Jiri Brus[d], Mohammed Jasim Uddin[e], Yasuhiko Hayashi[b], Okenwa Okoli[a,f], Tarik Dickens[a]

a. Industrial & Manufacturing Engineering, FAMU-FSU College of Engineering, 2525 Pottsdamer St., Tallahassee, Florida, 32310, USA.

b. Graduate School of Environmental, Life, Natural Science and Technology, Okayama University, 3-1-1 Tsushimanaka, Kita-ku, Okayama, 700-8530, Japan.

c. Department of Chemistry, Faculty of Science, Ain Shams University, 11566, Cairo, Egypt.

d. Institute of Macromolecular Chemistry of the Czech Academy of Sciences, Heyrovskeho nam. 2, 162 06, Prague 6, Czech Republic.

e. Photonic and Energy Research Laboratory, The University of Texas, Rio Grande Valley, 1201 West University Drive, Edinburg, Texas 78539, USA.

f. Herff College of Engineering, University of Memphis, Memphis, TN, 38111, USA.

Supporting Notes

Solid-state Nuclear Magnetic Resonance analysis

The ^{133}Cs and ^{1}H solid-state NMR spectra (ssNMR) were recorded at 11.7 T using a Bruker AVANCE III HD spectrometer and the 2.5 mm cross-polarization magic angle spinning (CP/MAS) probe operating at Larmor frequency of $\nu(^{133}Cs)$ = 65.611 MHz and $\nu(^{1}H)$ 500.180 MHz, respectively. All 1D MAS NMR experiments were collected at 27 kHz spinning speed without ^{1}H decoupling, using rotor synchronized spin-echo NMR experiments ($\pi/_2$-τ- π -acq.)[1], the delay between pulses was 1-loop for ^{133}Cs NMR experiment and 2-loops for ^{1}H NMR experiments, respectively. The recycle delay was 0.25 s for all ssNMR experiments and 100 s for selected samples. The number of scans was 8-8192. The ^{133}Cs chemical shift was calibrated using solid CsCl (^{133}Cs: 228.1 ppm)[2]. The pulse length was set to 2.6 µs at 130 W for maximal signal intensity. The final ^{133}Cs MAS NMR spectra are the sum of four sub-spectra recorded with steps of variable offset 1375 ppm. The ^{1}H chemical shift was calibrated using solid adamantane (^{1}H: 1.85 ppm)[3]. The pulse length was set to 1.5 µs at 97.65 W for $\pi/_2$ pulse. The ^{133}Cs spin-lattice relaxation times $T_1(^{133}Cs)$ were measured using the saturation recovery and inversion recovery experiments. The ^{133}Cs saturation recovery experiment was used to measure relatively long $T_1(^{133}Cs)$ relaxation times of ^{133}Cs species resonating at δ_{iso} = 64.4, 73.3, 146.4 and 152.5 ppm. In this experiment, prior to the read-out excitation $\pi/_2$ pulse (4 µs) and a variable delay ranging from 10 µs to 100 s (21 increments), the train of 200 saturation pulses (2.4 µs) spaced by 5 ms delays was used to saturate ^{133}Cs magnetization. Due to this saturation, a relatively short repetition delay of 4 s between the consecutive scans could be used. Consequently, the total experimental time of one experiment measured with 160 scans for each increment was 18 hours. The resonance offset was 500 ppm and the spectral width was 1200 ppm. On the other hand, because the train of pulses was unable to efficiently suppress the ^{133}Cs magnetization of the rapidly relaxing species resonating at 620 and 3100 ppm, the inversion recovery relaxation experiment had to be used to determine the corresponding ^{133}Cs spin-lattice relaxation times $T_1(^{133}Cs)$. The length of the initial π pulse was 15 µs at 200 W, and the variable delay covered the range of 10 µs to 0.25 s with 19 increments. To probe the relaxation time of the species resonating at 620 ppm the resonance offset, spectral width and the number of scans were set to 550 ppm, 1200 ppm and 144, respectively. Consequently, with the repletion delay of 4 s the total experimental time was 4 hours. To probe the relaxation time of the species resonating at 3100 ppm, the resonance offset, spectral width and the number of scans were set to 3000 ppm, 3000 ppm and 420, respectively. With the repletion delay of 4 s the total experimental time was then 9 hours. The single-component exponential function was used to simulate the obtained relaxation data. The build-up curves were constructed either from integrals or peak intensities of the corresponding signals, and the average values were calculated.

Supporting Figures

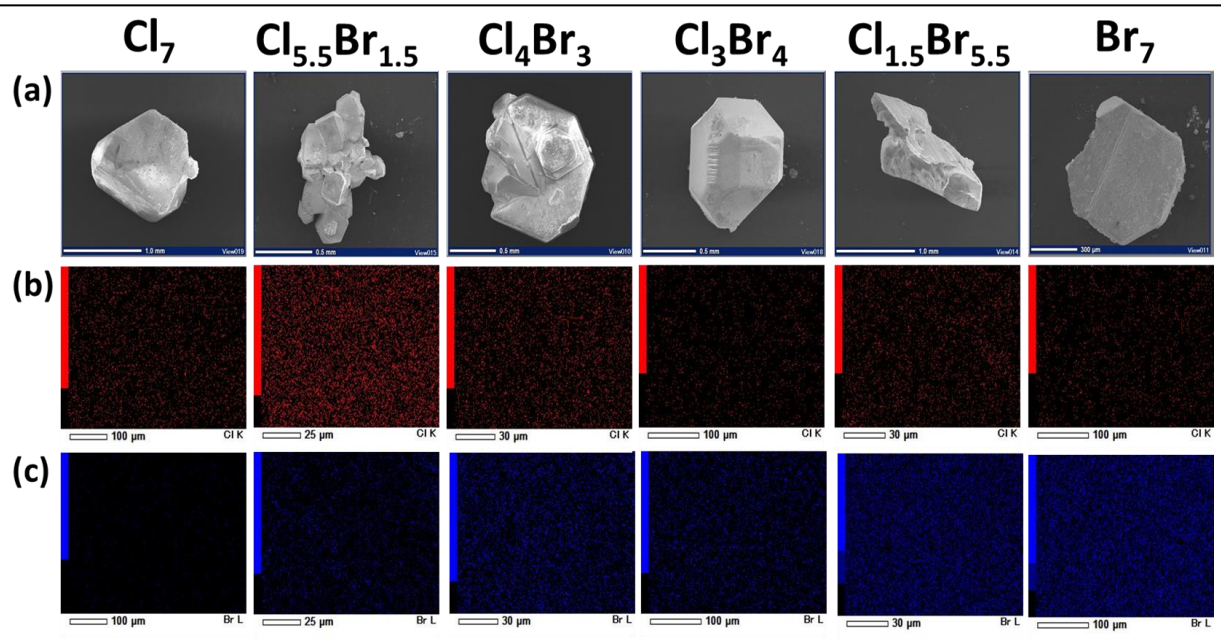

Fig. S1. SEM images (a) and EDS Mapping (b and c) of Cl and Br, respectively, for perovskite crystals.

.

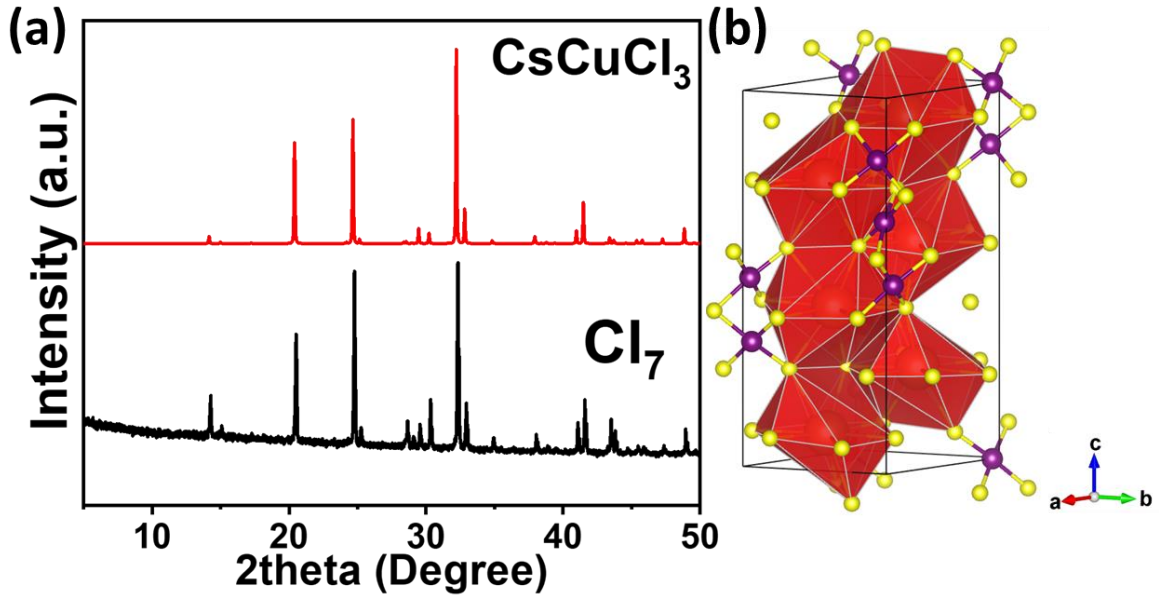

Fig. S2. Comparison of powder XRD measurement of Cl_7 perovskite powder with $CsCuCl_3$ perovskite. (b) Crystal structure of $CsCuCl_3$ perovskite (Structural data taken from ICSD No. 23959)[1].

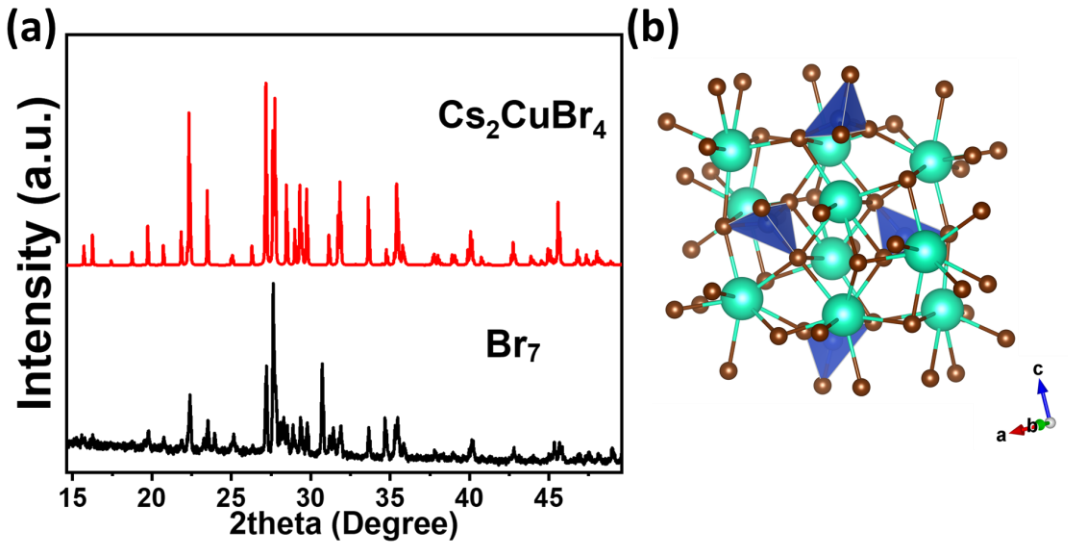

Fig. S3. Comparison of powder XRD measurement of Br_7 perovskite powder with Cs_2CuBr_4 perovskite. (b) Crystal structure of Cs_2CuBr_4 perovskite (Structural data taken from ICSD No. 169179)[4].

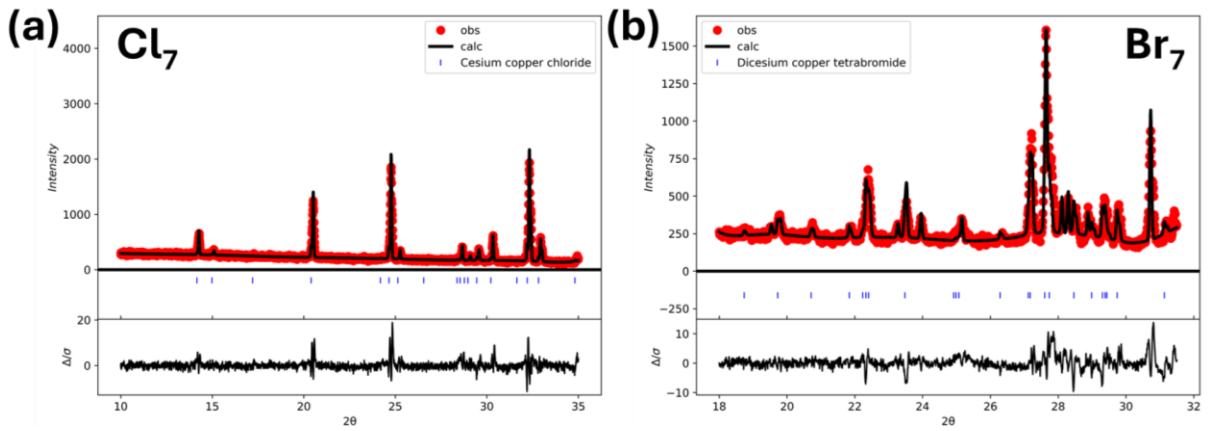

Fig. S4. Rietveld refinement of powder XRD patterns of Cl_7 (a) and Br_7 (b) mixed-cation copper perovskites.

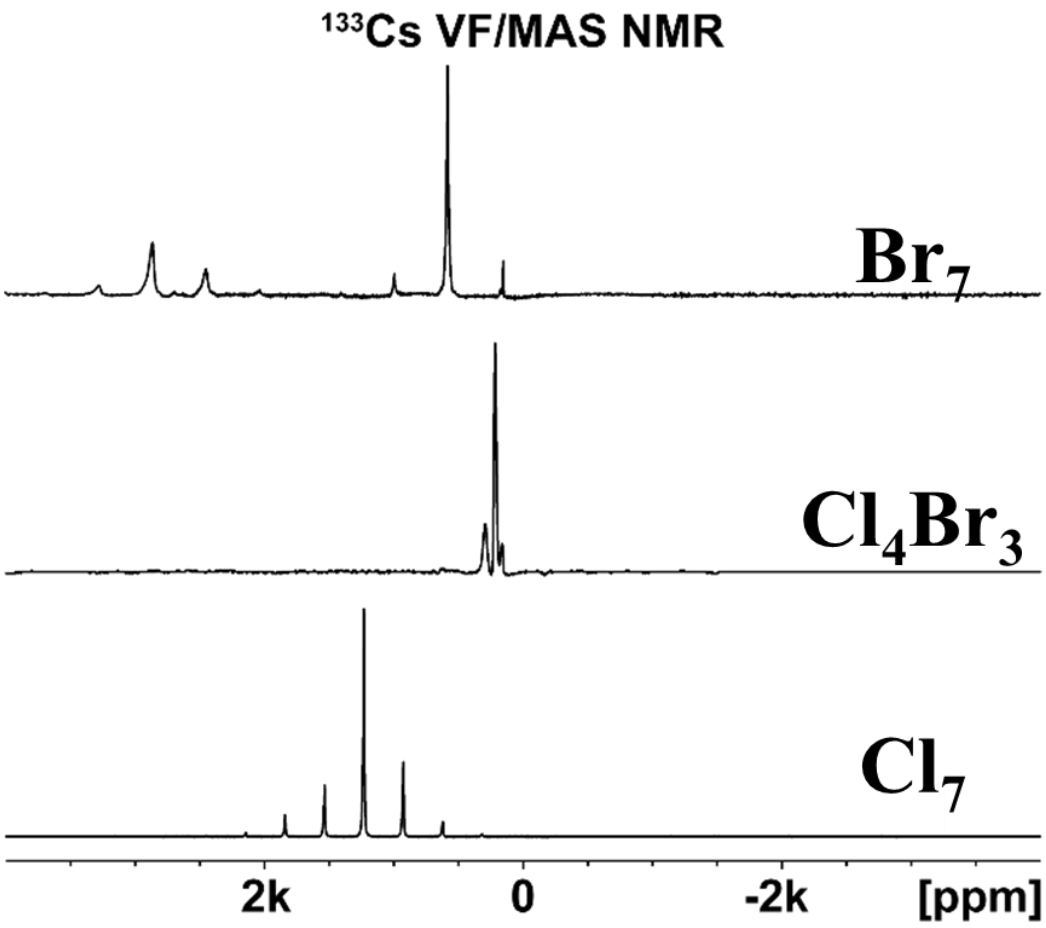

Fig. S5. Experimental ^{133}Cs VF/MAS NMR spectra of selected samples conducted at 27 kHz spinning speed of sample in spectral width 8000 ppm.

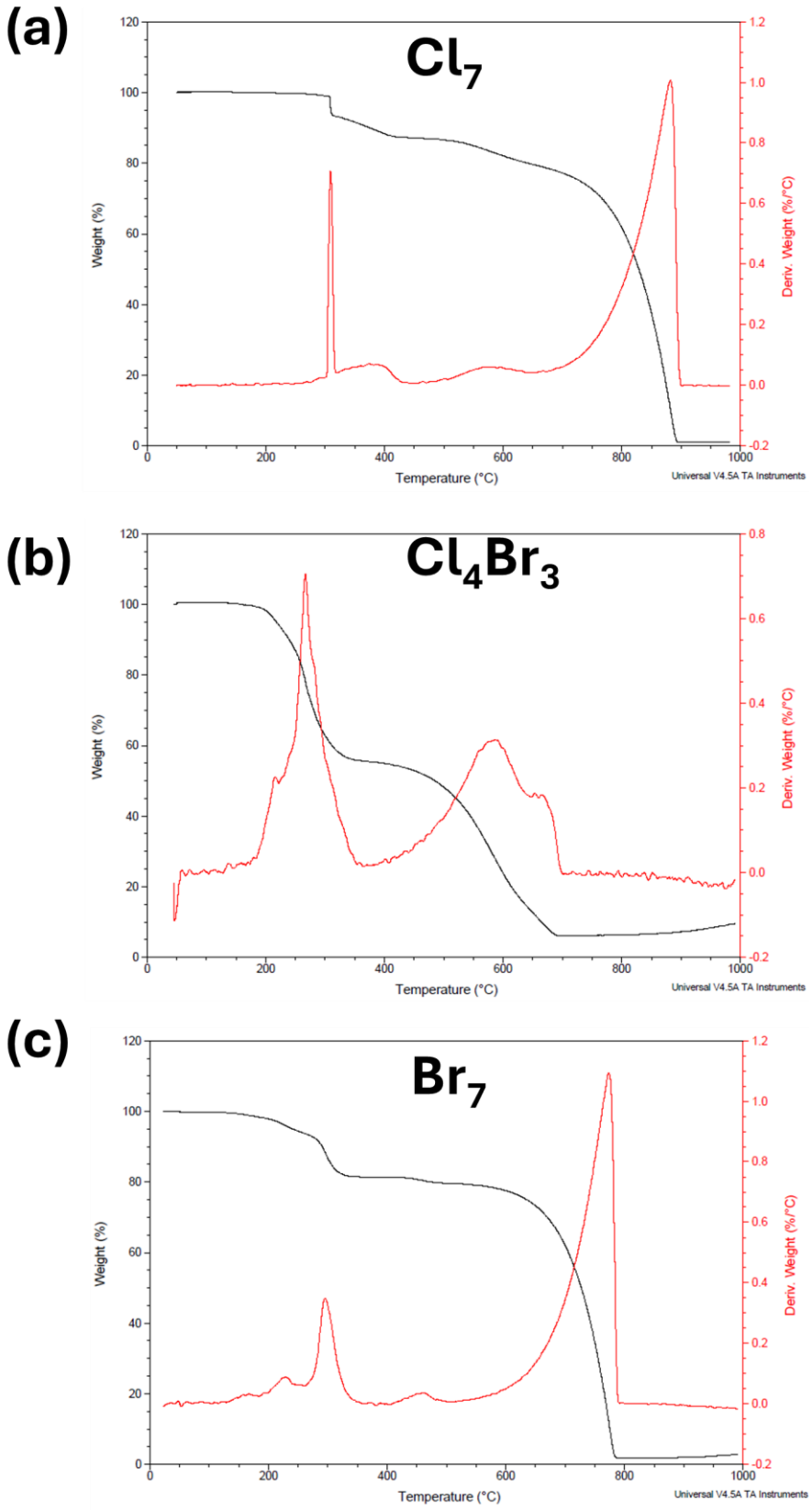

Fig. S6. Thermal stability measurement: Thermogravimetric analysis (TGA) of Cl_7 (a), Cl_4Br_3 (b), and Br_7 (c) perovskites, respectively.

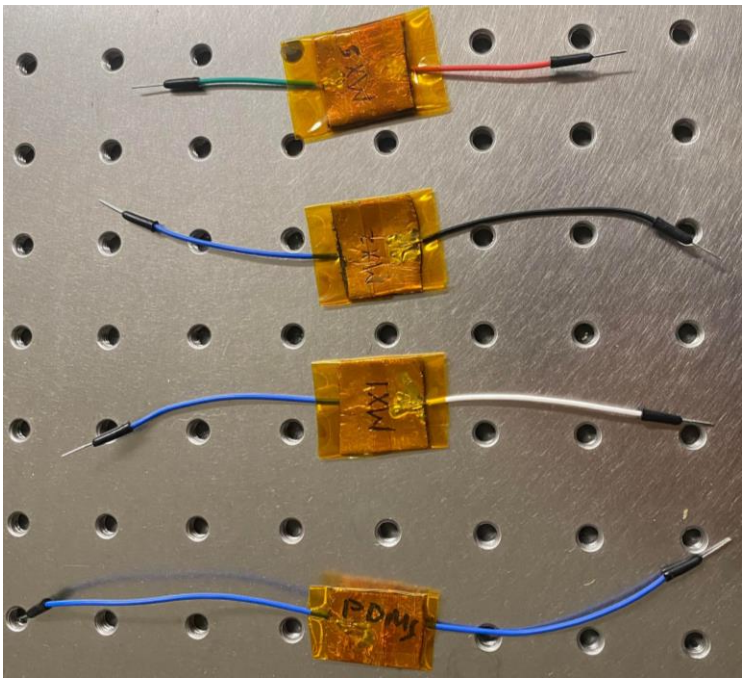

Fig. S7. Fabricated piezoelectric sensors: From bottom to top, PDMS only, Cl_7-PDMS, Br_7-PDMS, and Cl_4Br_3-PDMS perovskite-polymer composites, respectively.

Supporting Tables

Table S1. Comparison of output voltage of halide perovskites-based piezoelectric nanogenerators.

Halide perovskite	Polymer	Output voltage (V)	References
$FAPbBr_3$	PDMS	8	[5]
$MAPbI_3$	PDMS	2.7	[6]
$MASnI_3$	PVDF	12	[7]
MA_2CuCl_4	PVDF	4	[8]
$(MA/Cs)CuCl_4Br_3$	PDMS	5	This work

References

1 E. L. Hahn, *Physical Review*, 1950, **80**, 580–594.

2 A. R. Haase, M. A. Kerber, D. Kessler, J. Kronenbitter, H. Krüger, O. Lutz, M. Müller and A. Nolle, 1977, **32**, 952–956.

3 S. Hayashi and K. Hayamizu, *Bull Chem Soc Jpn*, 1991, **64**, 685–687.

4 N. Krüger, S. Belz, F. Schossau, A. A. Haghighirad, P. T. Cong, B. Wolf, S. Gottlieb-Schoenmeyer, F. Ritter and W. Assmus, *Cryst Growth Des*, 2010, **10**, 4456–4462.

5 R. Ding, H. Liu, X. Zhang, J. Xiao, R. Kishor, H. Sun, B. Zhu, G. Chen, F. Gao, X. Feng, J. Chen, X. Chen, X. Sun and Y. Zheng, *Adv Funct Mater*, 2016, **26**, 7708–7716.

6 Y.-J. Kim, T.-V. Dang, H.-J. Choi, B.-J. Park, J.-H. Eom, H.-A. Song, D. Seol, Y. Kim, S.-H. Shin, J. Nah and S.-G. Yoon, *J Mater Chem A Mater*, 2016, **4**, 756–763.

7 S. Ippili, V. Jella, J.-H. Eom, J. Kim, S. Hong, J.-S. Choi, V.-D. Tran, N. Van Hieu, Y.-J. Kim, H.-J. Kim and S.-G. Yoon, *Nano Energy*, 2019, **57**, 911–923.

8 S. Huang, G. Tang, H. Huang, X. Wu, P. Zhou, L. Zou, L. Xie, J. Deng, X. Wang, H. Zhong and J. Hong, *Sci Bull (Beijing)*, 2018, **63**, 1254–1259.